Article

SOURCE DATA | TRANSPARENT PROCESS

THE EMBO JOURNAL

A combination of Wnt and growth factor signaling induces Arl4c expression to form epithelial tubular structures

Shinji Matsumoto[1], Shinsuke Fujii[1,2], Akira Sato[1], Souji Ibuka[1,3], Yoshinori Kagawa[4,5,6], Masaru Ishii[5,6] & Akira Kikuchi[1,*]

Abstract

Growth factor-dependent epithelial morphological changes and proliferation are essential for the formation of tubular structures, but the underlying molecular mechanisms are poorly understood. Co-stimulation with Wnt3a and epidermal growth factor (Wnt3a/EGF) induced development of tubes consisting of intestinal epithelial cells by inducing expression of Arl4c, an Arf-like small GTP-binding protein, in three-dimensional culture, while stimulation with Wnt3a or EGF alone did not. Arl4c expression resulted in rearrangement of the cytoskeleton through activation of Rac and inactivation of Rho properly, which promoted cell growth by inducing nuclear translocation of Yes-associated protein and transcriptional co-activator with PDZ-binding motif (YAP/TAZ) in leading cells. Arl4c was expressed in ureteric bud tips and pretubular structures in the embryonic kidney. In an organoid culture assay, Wnt and fibroblast growth factor signaling simultaneously induced elongation and budding of kidney ureteric buds through Arl4c expression. YAP/TAZ was observed in the nucleus of extending ureteric bud tips. Thus, Arl4c expression induced by a combination of growth factor signaling mechanisms is involved in tube formation.

Keywords epithelium; growth factor; tubulogenesis; Wnt; YAP
Subject Categories Cell Adhesion, Polarity & Cytoskeleton; Development & Differentiation
DOI 10.1002/embj.201386942 | Received 23 September 2013 | Revised 13 January 2014 | Accepted 14 January 2014 | Published online 21 February 2014
EMBO J (2014) 33, 702–718

Introduction

Epithelial tube-like structures are basic, common units in various organs, including salivary glands, lungs, mammary glands, guts, pancreas, the liver, and kidneys (Gumbiner, 1992). In epithelial tubes, cells are interconnected by intercellular junctions to form a cylindrical structure and are polarized with apical and basolateral surfaces (O'Brien *et al*, 2002). Cysts are spherical monolayers of cells that enclose a central lumen. Although they are considered topologically equivalent to tubes, they are immotile and less proliferative. Growth factor signaling causes cysts to develop branching tubes. Madin Darby canine kidney (MDCK) cysts are a well-established model for tubulogenesis in that the cysts tubulate in three-dimensional (3D) culture in response to hepatocyte growth factor (HGF) (O'Brien *et al*, 2002; Debnath & Brugge, 2005; Tushir & D'Souza-Schorey, 2007). Activation of the receptor tyrosine kinase Met by HGF leads to induction of changes in cell morphology, motility, and proliferation during tube formation, but the mechanisms connecting the individual events are not well understood (Rosario & Birchmeier, 2003). As another model, epithelial rudiments isolated from tubular organs such as the lungs, kidneys, and salivary glands were able to change their morphology and undergo tube formation by various growth factors in a 3D basement membrane matrix (BMM) such as Matrigel (Ohtsuka *et al*, 2001; Steinberg *et al*, 2005; Zhang *et al*, 2012), but the detailed mechanisms underlying organ tubulogenesis are only partially understood. Therefore, a new *in vitro* approach in which epithelial cells develop tubes in a 3D BMM is necessary for understanding the common signaling pathway regulating tubulogenesis *in vivo*.

Herein, we show that in cooperation with the growth factor-MAP kinase (MAPK) pathway, the Wnt3a-β-catenin pathway regulates the morphology, motility, and proliferation of cultured intestinal epithelial cells through expression of ADP-ribosylation factor (Arf)-like 4C (Arl4c), resulting in tube formation in 3D Matrigel culture (3D culture). Simultaneous stimulation with Wnt3a and epidermal growth factor (EGF) induced Arl4c expression by forming a complex between Ets, T-cell factor 4 (Tcf4), and cyclic AMP-responsive element binding protein (CREB)-binding protein (CBP) at the

1 Department of Molecular Biology and Biochemistry, Graduate School of Medicine, Osaka University, Osaka, Japan
2 Interdisciplinary Program for Biomedical Sciences (IPBS), Institute for Academic Initiatives, Osaka University, Graduate School of Medicine, Osaka, Japan
3 Department of Pediatric Surgery, Graduate School of Medicine, Osaka University, Osaka, Japan
4 Department of Gastrointestinal Surgery, Graduate School of Medicine, Osaka University, Osaka, Japan
5 Department of Immunology and Cell Biology, Graduate School of Medicine, Osaka University, Osaka, Japan
6 Japan Science and Technology Agency (JST), CREST, Tokyo, Japan
*Corresponding author. Tel: +81 6 6879 3410; Fax: +81 6 6879 3419; E-mail: akikuchi@molbiobc.med.osaka-u.ac.jp

Ets-binding site of the Arl4c gene. Arl4c expression activated Rac1 through Arf6, resulting in inhibition of RhoA. We also demonstrate that Arl4c expression is involved in elongation and budding of kidney ureteric buds (UBs), suggesting the existence of a common mechanism regulating tube formation.

Results

Intestinal epithelial cell tube formation in response to Wnt3a and EGF

We examined whether cultured epithelial cells induce tube development in 3D culture in response to various growth factors and found rat intestinal epithelial cells 6 (IEC6) to be a useful model. IEC6 formed small spherical cysts in 3D culture (Fig 1A). Wnt has been reported to be required for elongation of tubes and branching morphogenesis in mice knockout studies (van Amerongen & Berns, 2006; Miller & McCrea, 2010), but the underlying mechanism for Wnt-regulated tubulogenesis remains unclear. Among the 19 Wnt family members, Wnt3a and Wnt5a activate the β-catenin-dependent and β-catenin-independent pathways, respectively (Kikuchi *et al*, 2011). HGF, Wnt3a, or Wnt5a alone did not affect morphogenesis of IEC6 cysts in 3D culture, and EGF alone enlarged the cysts and occasionally induced formation of small protrusions from the cysts (Fig 1A; Supplementary Fig S1A and B). Simultaneous stimulation of IEC6 cells with Wnt3a and EGF (Wnt3a/EGF) or HGF (Wnt3a/HGF) resulted in formation of branched tubular structures (Fig 1A and B), but Wnt5a/EGF showed enlargement of cysts, which is similar to treatment with EGF alone and Wnt5a/HGF did not affect cyst morphology (Supplementary Fig S1A). IEC6 cells expressed high levels of Wnt5a, and knockdown of Wnt5a suppressed Rac1 activity and lead to loss of lumen integrity with fragmented apical and disrupted basolateral structures (Gon *et al*, 2013). Given that endogenous Wnt5a is sufficient to regulate the functions of IEC6 cells, the cells may not respond to exogenous Wnt5a. The tubes had continuous lumens with apical markers (F-actin, phospho-ezrin, ezrin, and aPKC) and basolateral markers (β-catenin and E-cadherin) (Fig 1A and B; Supplementary Fig S1C), indicating that IEC6 cells are polarized along the apicobasal axis.

The numbers of tubes extending from a main trunk in response to growth factors were evaluated as an indicator of tube formation (Supplementary Fig S1D and E). This reflects the length of tubes and extent of branching. Because Wnt3a/EGF promotes tube formation more efficiently than Wnt3a/HGF (Supplementary Fig S1E), IEC6 cells were treated with Wnt3a/EGF in the following experiments. In this method, IEC6 cells were treated with growth factors at the same time the cells were placed on Matrigel. As a second method, IEC6 cells were treated with growth factors after they formed cysts in 3D culture. Under the latter conditions, cysts did not develop tubes following stimulation with Wnt3a, EGF, or HGF alone. Tube formation from cysts was induced by Wnt3a/EGF, although efficiency was lower compared with the former method (Supplementary Fig S2). Wnt3a is an insoluble protein and readily attached to extracellular matrix (ECM) components, including proteins and glycans, through lipid and glycan modifications of Wnts (Sakane *et al*, 2012; Yamamoto *et al*, 2013). Therefore, Wnt3a may not be easily accessible to IEC6 cysts embedded in 3D culture, which may be a reason for low tubulogenesis efficiency by the latter method.

The tube formation process of IEC6 cells by Wnt3a/EGF is similar to that of HGF-induced tube formation of MDCK cells (O'Brien *et al*, 2002; Bryant & Mostov, 2008) (Fig 1B). It begins with cytoplasmic extension of some cells into the surrounding matrix. In the second stage of tubulogenesis, single-file chains develop linearly. Chains subsequently transform into multilayered cords by promoting proliferation, in which discontinuous lumens are visible. During the maturation process from cords to tubes, cells in the cords are polarized to generate cylindrical tubes. To examine morphological and cytoskeletal changes in IEC6 cells by Wnt3a/EGF, cells were grown on a Matrigel-coated dish two-dimensionally (2D culture) and stained with phalloidin and anti-phospho-myosin-light chain2 (ppMLC2) (Thr18/Ser19) antibody. IEC6 cells were spread out, and cortical actin and stress fibers were observed (Fig 1C). Treatment with Wnt3a or EGF alone did not affect cell morphology, whereas Wnt3a/EGF changed cell morphology, resulting in long cytoplasmic extension of cells with multiple lamellipodia (Fig 1C and D). Actinomycin D inhibited Wnt3a/EGF-dependent morphological changes and expression of Axin2, a target gene of Wnt signaling (Supplementary Fig S3A and B), suggesting that these morphological changes are a result of gene expression.

Arl4c expression is involved in Wnt3a/EGF-induced tube formation

DNA microarray analyses were performed at 4 and 24 h after stimulation with Wnt3a, EGF, or Wnt3a/EGF in 3D culture. Candidate genes were selected based on the criterion that expression levels were higher in cells treated with Wnt3a/EGF than in cells treated with either Wnt3a or EGF at both time points (Supplementary Table S1). Of two possible candidate genes, Arl4c, which belongs to the Arf-related small GTP-binding family and of which functions are not yet understood (Burd *et al*, 2004), was further analyzed. Wnt3a/EGF more than additively increased Arl4c mRNA and protein levels in IEC6 cells (Fig 1E). In 2D culture, endogenous Arl4c expressed by Wnt3a/EGF was localized to the leading edge of elongated IEC6 cells where F-actin was also accumulated (Supplementary Fig S3C). Knockdown of Arl4c suppressed Wnt3a/EGF-dependent morphological changes, and human Arl4c expression induced cell extension in the presence of EGF alone (Supplementary Fig S3D–F).

In 3D culture, knockdown of Arl4c did not affect the morphology of IEC6 cysts, but inhibited the elongation and branching of tubes induced by Wnt3a/EGF (Fig 1F). Among the processes of tube formation, "extension" was significantly inhibited (Supplementary Fig S4A). This could reflect the ability of Arl4c to regulate the actin cytoskeleton at initiation of tubulogenesis. Human Arl4c expression rescued the phenotypes induced by siRNA, excluding siRNA off-target effects (Fig 1F; Supplementary Fig S4B and C). Furthermore, expression of Arl4c-GFP, but not Arl4c^{T27N}-GFP (a GDP-restricted mutant of Arl4c), increased the number of extended structures in the presence of EGF (Fig 1G; Supplementary Fig S4D). These results suggest that Arl4c expression induced by Wnt3a/EGF is involved in changes in cell morphology and tube formation.

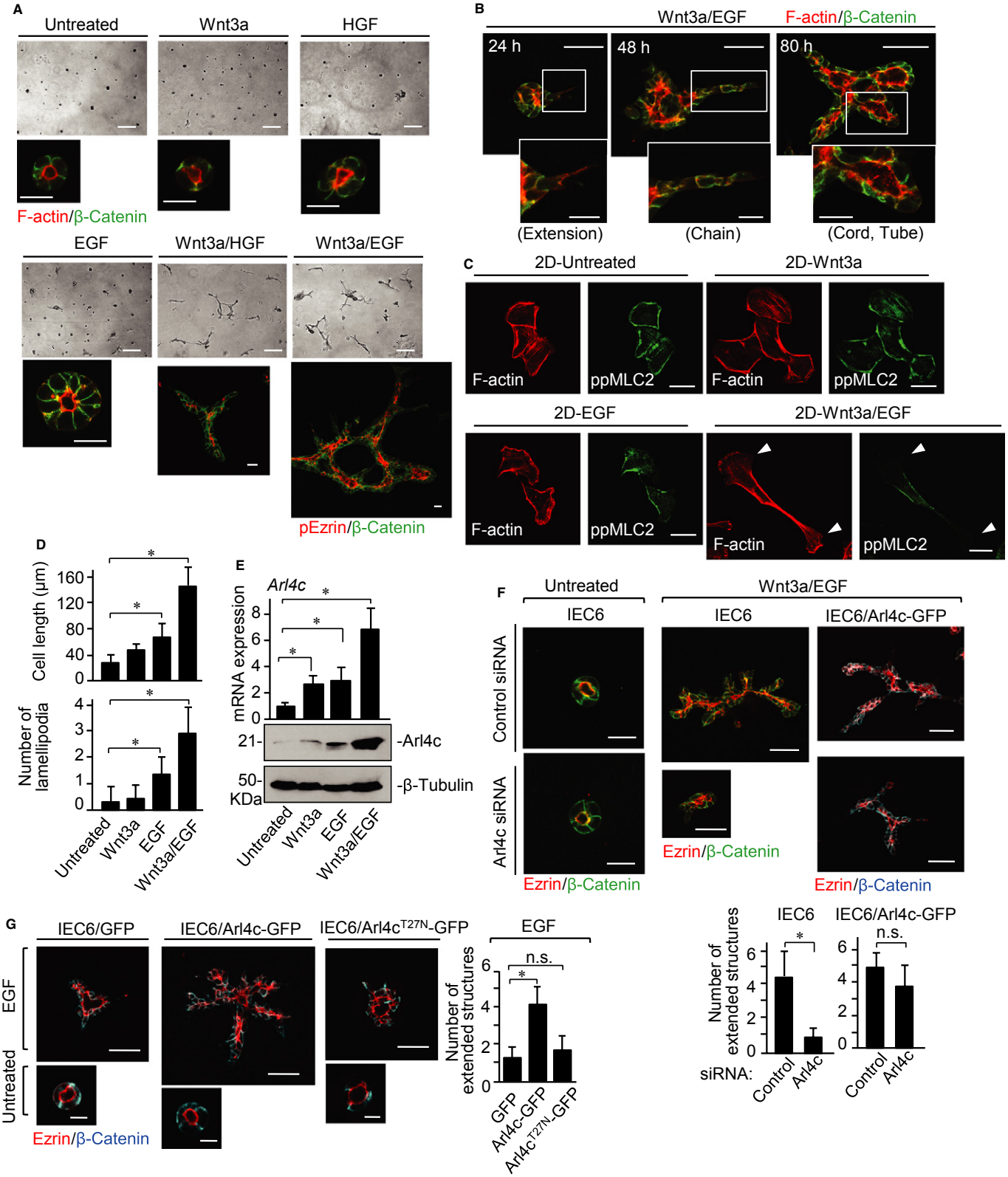

Apoptosis has been implicated in luminal formation of salivary or mammary glands and MCF-10A mammary epithelial cells (Hoffman *et al*, 1996; Korff & Augustin, 1998; Debnath *et al*, 2002). Cysts and tubes consisting of IEC6 cells were stained with anti-active caspase-3 antibody (Supplementary Fig S4E). Active caspase-3-positive cells (apoptotic cells) were observed in the luminal space

Figure 1. Arl4c expression is required for tube formation of IEC6 cells in 3D culture.

A IEC6 cells were cultured under the indicated conditions for 72 h in 3D Matrigel. Cells were photographed using phase contrast microscopy and stained with the indicated antibodies or phalloidin.

B IEC6 cells were cultured with Wnt3a and epidermal growth factor (Wnt3a/EGF) for 24, 48, or 80 h in 3D Matrigel and stained with anti-β-catenin antibody and phalloidin.

C, D IEC6 cells grown on a Matrigel-coated coverslip (2D culture) were cultured under the indicated conditions for 18 h and stained with the indicated antibody and phalloidin. White arrowheads indicate lamellipodia (C). The length of the long axis and the number of lamellipodia of cells were measured per treatment (n = 50) (D).

E IEC6 cells were stimulated as indicated for 18 h. Real-time PCR analyses for *Arl4c* mRNA expression were performed. The results are expressed as fold increase compared with *Arl4c* mRNA levels in untreated cells. Whole lysates were probed with the indicated antibodies.

F IEC6 cells or IEC6 cells stably expressing Arl4c-GFP (IEC6/Arl4c-GFP) were transfected with control or Arl4c siRNA and cultured with or without Wnt3a/EGF for 60 h. The cells were stained with the indicated antibodies. The number of extended structures from multicellular trunks was counted (n = 30).

G IEC6 cells stably expressing GFP, Arl4c-GFP, or Arl4c^{T27N}-GFP were cultured with or without EGF for 60 h and stained with the indicated antibodies.

Data information: Results are shown as the mean ± SE from three independent experiments. Scale bars in (A), 200 μm (top panels) and 20 μm (bottom panels); in (B), 50 μm (top panels) and 20 μm (bottom panels); in (C), 20 μm; in (F), 20 μm (left two panels) and 50 μm (right four panels); in (G), 50 μm (top panels) and 10 μm (bottom panels). *P < 0.01; n.s., not significant.

Source data are available online for this figure.

of IEC6 cysts and in the interior of developing tubes induced by Wnt3a/EGF. These nuclei were abnormally shaped. IEC6 cells forming cysts and tubes were caspase-3 negative, with intact nuclei. Knockdown of Arl4c did not increase apoptotic cells in the luminal space of cysts compared with control (Supplementary Fig S4E and F), suggesting that depletion of Arl4c did not affect cell viability.

Wnt3a/EGF induces Arl4c expression through the β-catenin and MAPK pathways

We examined the mechanism by which Wnt3a/EGF induces Arl4c expression. Wnt3a/EGF-induced Arl4c mRNA expression was reduced by knockdown of β-catenin (Fig 2A; Supplementary Fig S5A) and overexpression of a dominant negative form of Tcf4 (DN-Tcf4) (Supplementary Fig S5B). EGF activates various signaling cascades, including the Ras-Raf-MAPK, PI-3 kinase-AKT, and protein kinase C (PKC)-c-Jun N-terminal kinase (JNK) pathways (Avraham & Yarden, 2011). U0126 (a MEK inhibitor) inhibited Wnt3a/EGF-induced Arl4c mRNA expression in IEC6 cells more efficiently compared with wortmannin (a PI-3 kinase inhibitor) and SP600125 (a JNK inhibitor) (Fig 2B). The Ets family acts as transcription factors downstream of MAPK (Garrett-Sinha, 2013). Knockdown of Ets1/2, but not Elk1, suppressed Wnt3a/EGF-induced Arl4c mRNA expression (Fig 2C; Supplementary Fig S5C). Wnt3a/EGF-induced upregulation of Arl4c mRNA was also observed in HeLaS3 cells (Supplementary Fig S5D). Simultaneous expression of SA-β-catenin (an active form of β-catenin) and Raf-CAAX (an active form of Raf) in HeLaS3 cells synergistically stimulated Arl4c mRNA expression (Supplementary Fig S5E). The combination of CHIR99021, which activates the β-catenin-dependent pathway (Ring *et al*, 2003), and EGF also synergistically increased Arl4c mRNA levels in IEC6 cells (Supplementary Fig S5F). Thus, Wnt3a/EGF induces Arl4c expression coordinately through the β-catenin and MAPK pathways.

We found putative Ets- and lymphocyte enhancement factor 1 (LEF1)-binding sites in the 3′ untranslated region (UTR) of the human Arl4c gene by using ECR Browse (Fig 2D). The sites were conserved in mouse and rat Arl4c genes. Reporter assays revealed that genomic regions +2965 to +3690 and +2965 to +3164, but not +3195 to +3690, in mice activate transcriptional activity by activating both the β-catenin and MAPK pathways (Fig 2E). Chromatin immunoprecipitation assay showed that Ets1 consistently binds to the rat genomic region equivalent to mouse +2965 to +3164 and also revealed that EGF promotes formation of a complex between Tcf4, CBP, and the Ets-binding region (Fig 2F). CHIR99021/EGF further enhanced the association of Tcf4 and CBP with the Ets-binding region, in which acetylation of lysine 8 in histone H4 (H4K8) was also enhanced (Fig 2F). In addition, Ets1 formed a complex with Tcf4 without stimulation, and this binding was enhanced by treatment with CHIR99021 alone or CHIR99021/EGF (Fig 2G). β-catenin was also observed in this complex (Fig 2G). When DN-Tcf4, which lacks the β-catenin-binding site, was expressed instead of wild-type HA-Tcf4, DN-Tcf4, and β-catenin were not associated with Ets1 (Supplementary Fig S5G), suggesting that the β-catenin/Tcf4 complex is able to interact with Ets1 and that Tcf4 binds to β-catenin and Ets1 through the different sites. These results suggest that the EGF-MAPK pathway induces the interaction of the β-catenin/Tcf4 complex with Ets1 and the Wnt3a-β-catenin pathway enhances it. Therefore, Wnt3a/EGF induces Arl4c expression through the β-catenin/Tcf4/Ets1 complex, which recruits histone acetyltransferase CBP.

Consistent with these results, knockdown of low-density lipoprotein receptor-related protein (LRP) 5 and LRP6, Dishevelled1 (Dvl1), Dvl2, and Dvl3, or β-catenin, which are major components of the β-catenin pathway, decreased the number of extended tube structures induced by Wnt3a/EGF (Fig 2H; Supplementary Fig S5H). Tube formation was also inhibited by treatment with IWR1, a Wnt signal inhibitor (Chen *et al*, 2009), or DN-Tcf4 expression (Fig 2H). CHIR99021 alone did not affect cyst morphology, and CHIR99021/EGF increased the number of extended tube structures (Supplementary Fig S5I). U0126 or knockdown of Ets1/2 decreased Wnt3a/EGF-induced tube formation (Fig 2H). These gain- and loss-of-function experiments suggest that the β-catenin and MAPK pathways are necessary and sufficient for Wnt3a/EGF-induced Arl4c expression and tube formation.

Arl4c regulates Rac and Rho activities

We focused on identifying signaling pathways modulated by Arl4c. Arl4c-GFP expression in IEC6 cells induced F-actin-rich membrane ruffles where Arl4c-GFP was localized, but Arl4c^{T27N}-GFP was distributed throughout the cytosol and did not affect cell morphology

(Supplementary Fig S6A). As shown in Fig 1C, Wnt3a/EGF promoted induction of multiple lamellipodia, suggesting that Rac is activated. Stimulation of IEC6 cells with Wnt3a/EGF for 18 h increased Rac1 activation compared with either Wnt3a or EGF (Fig 3A). Arl4c expression activated Rac1, and its depletion inhibited Wnt3a/EGF-dependent activation of Rac1 (Fig 3B), indicating that Arl4c functions upstream of Rac1. It was reported that Arl4c binds to Arf nucleotide-binding site opener (ARNO), which activates Arf6 (Hofmann *et al*, 2007), and that Arf6 activates Rac through Kalirin and the DOCK180/Elmo complex (Santy *et al*, 2005; Koo *et al*, 2007). Consistently, Wnt3a/EGF activated Arf6 compared with either Wnt3a or EGF (Supplementary Fig S6B), and treatment with SecinH3 (an ARNO inhibitor) (Hafner *et al*, 2006) or knockdown of Arf6 inhibited Arl4c- and Wnt3a/EGF-dependent Rac1 activation (Fig 3B; Supplementary Fig S6C). Thus, Wnt3a/EGF-dependent Rac1 activation could be mediated by Arl4c.

MLC2 phosphorylation was clearly visible along the longitudinal axis of cells extended by Wnt3a/EGF, but it was reduced around lamellipodia (see Fig 1C), suggesting local inhibition of Rho activity. Wnt3a/EGF significantly reduced MLC2 phosphorylation and RhoA activity compared with either Wnt3a or EGF alone (Fig 3C and D). Knockdown of Arl4c partially restored Wnt3a/EGF-induced inhibition of RhoA activity (Fig 3D). Activation of Rac was shown to inhibit Rho activity in melanoma cells (Sanz-Moreno *et al*, 2008). Consistent with the report, expression of Arl4c-GFP or a constitutively active form of Rac1 ($Rac1^{G12V}$) indeed inhibited RhoA in IEC6 cells (Fig 3E; Supplementary Fig S6D), suggesting that RhoA functions downstream of Arl4c and Rac1 in the cells. Thus, Wnt3a/EGF-induced Arl4c expression resulted in regulation of Rac and Rho activities through ARNO and Arf6.

To examine whether this signaling axis is involved in Wnt3a/EGF-induced tube formation, IEC6 cells were treated with pharmacological and genetic manipulations in 2D and 3D culture. In 2D culture, Wnt3a/EGF-induced cell extension and lamellipodia formation were inhibited by knockdown of ARNO or Arf6 and by treatment with SecinH3 or NSC23766 (a Rac inhibitor) (Gao *et al*, 2004) (Supplementary Fig S7A). Y27632 (a Rho-kinase inhibitor) or blebbistatin (an ATPase inhibitor of myosin heavy chain) (Straight *et al*, 2003) induced cell extension in the presence of EGF but not Wnt3a (Supplementary Fig S7B), suggesting that Rho inhibition mimics Wnt3a signaling.

In 3D culture, Wnt3a/EGF-induced tube formation was inhibited by knockdown of ARNO or Arf6, treatment with SecinH3 or NSC23766, or expression of $Rac1^{T17N}$ (a dominant negative form of Rac1) or $Arf6^{T27N}$ (a dominant negative form of Arf6) (Fig 3F; Supplementary Fig S7C and D). Arf6 expression rescued the phenotypes in Arf6-depleted cells (Supplementary Fig S7E). Active caspase-3-positive cells with abnormal nuclei were observed in the interior of the luminal space of tubes treated with SecinH3 and NSC23766, but the treatment did not increase the number of apoptotic cells compared with control, suggesting that the inhibitors do not affect viability of IEC6 cells forming cysts and tubes (see Supplementary Fig S4E and G). NSC23766 or SecinH3 also inhibited tube formation in Arl4c-GFP-expressing IEC6 cells treated with EGF (Fig 3G).

Co-stimulation with EGF and 2 μM Y27632 or blebbistatin developed tubular structures (Fig 3H). However, when IEC6 cells were treated with 100 μM Y27632 or 25 μM blebbistatin in the presence of EGF, the cells rarely developed tubes (Fig 3H). Therefore, severe inhibition of actomyosin contraction does not contribute to tube formation. These results suggest that Wnt3a/EGF activates Rac and inhibits Rho properly through Arl4c expression, resulting in rearrangement of actomyosin to induce changes in cell morphology and tube development.

Arl4c is linked to cell proliferation through nuclear localization of YAP/TAZ

When IEC6 cells expressing Arl4c-GFP were mixed with control IEC6 cells at a ratio of 1:1, Arl4c-GFP-positive cells tended to be located at the extended structures where cells were elongated (Fig 4A). In addition to changes in cell morphology, epithelial cells must proliferate to form tubes (see Fig 1B). To analyze spatiotemporal regulation of cell proliferation in tube formation, we generated IEC6 cells expressing a fluorescent, ubiquitination-based cell cycle indicator (Fucci) construct (Sakaue-Sawano *et al*, 2008). In the Fucci system, cells with red and green nuclei indicate G1 (less proliferative) and S/G2/M (proliferative) phases, respectively (Supplementary Fig S8A). Cells had green, red, yellow, or colorless nuclei

Figure 2. Wnt3a and epidermal growth factor (Wnt3a/EGF) induces Arl4c expression through β-catenin and MAP kinase (MAPK) pathways.

A IEC6 cells transfected with β-catenin siRNA were stimulated with Wnt3a/EGF for 8 h. Real-time PCR analyses for *Arl4c* mRNA expression were performed.

B IEC6 cells were treated with or without U0126, SP600125, or wortmannin for 1 h and stimulated with Wnt3a/EGF for 8 h to measure *Arl4c* mRNA levels.

C IEC6 cells transfected with siRNAs against Elk1 or Ets1 and 2 were stimulated with Wnt3a/EGF for 8 h to measure *Arl4c* mRNA levels.

D Arl4c-luciferase constructs used in this study are shown. The *Arl4c* gene contains predicted ETS- and LEF1-binding sites in the 3′ untranslated region (UTR), position around 3 kb from the transcription start site.

E After HeLaS3 cells were transfected with the indicated constructs, luciferase activities were measured and expressed as fold increase compared with constructs expressing GFP.

F Chromatin from IEC6 cells treated as indicated was immunoprecipitated with indicated antibodies. The precipitated *Arl4c* 3′-UTR was analyzed by PCR with region-specific primers.

G HeLaS3 cells were treated with CHIR99021/EGF for 3 h, and lysates were immunoprecipitated with anti-Ets1 antibody. Immunoprecipitates were probed with the indicated antibodies.

H IEC6 cells transfected with the indicated siRNAs, cells stably expressing a dominant negative form of Tcf4 (DN-Tcf4), or cells treated with IWR1 or U0126 were stimulated with Wnt3a/EGF for 60 h in 3D culture and stained with anti-β-catenin antibody and phalloidin. The number of extended structures from multicellular trunks was counted (n = 30).

Data information: Results are shown as the mean ± SE from three independent experiments. Scale bars in (H), 50 μm. *$P < 0.01$

Source data are available online for this figure.

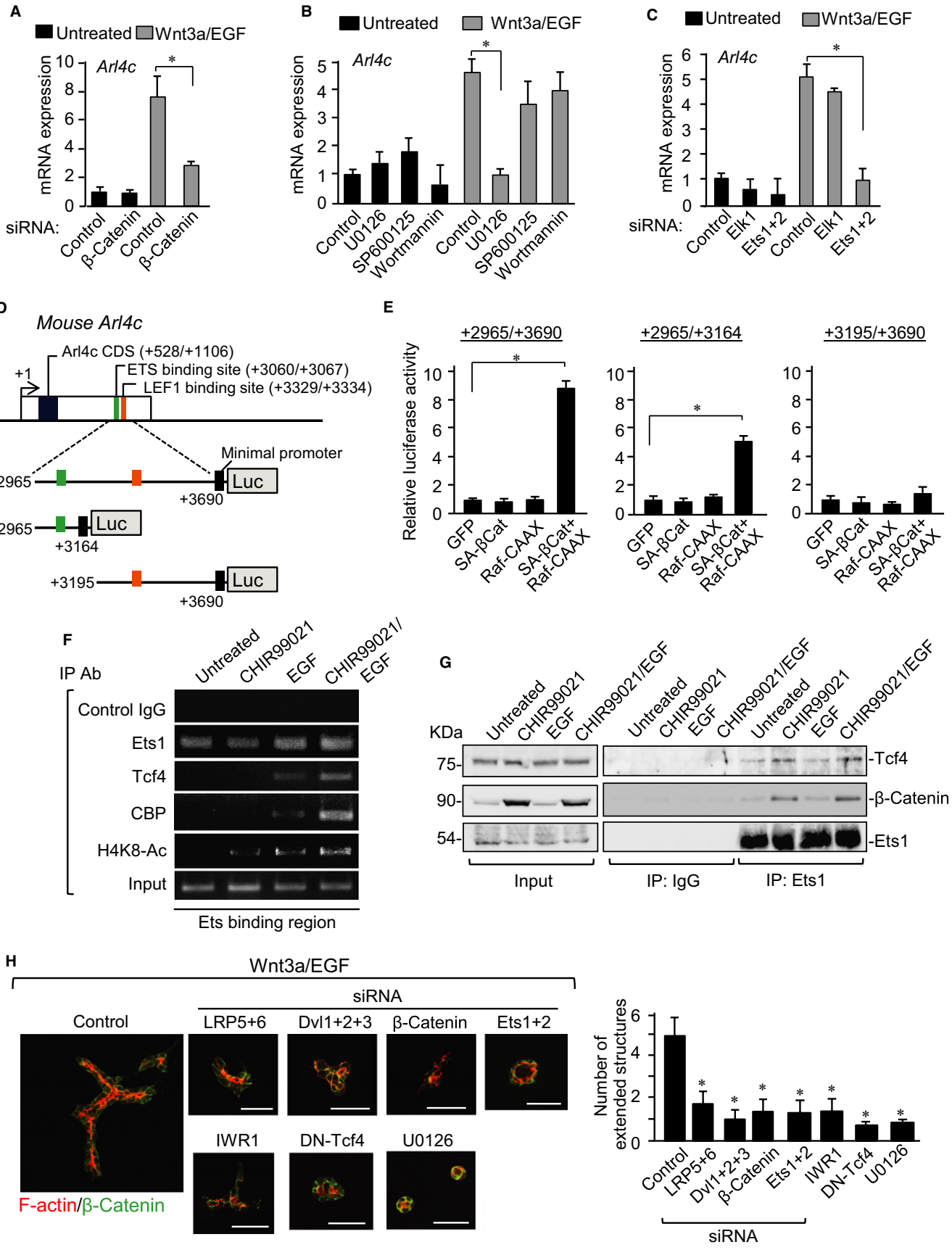

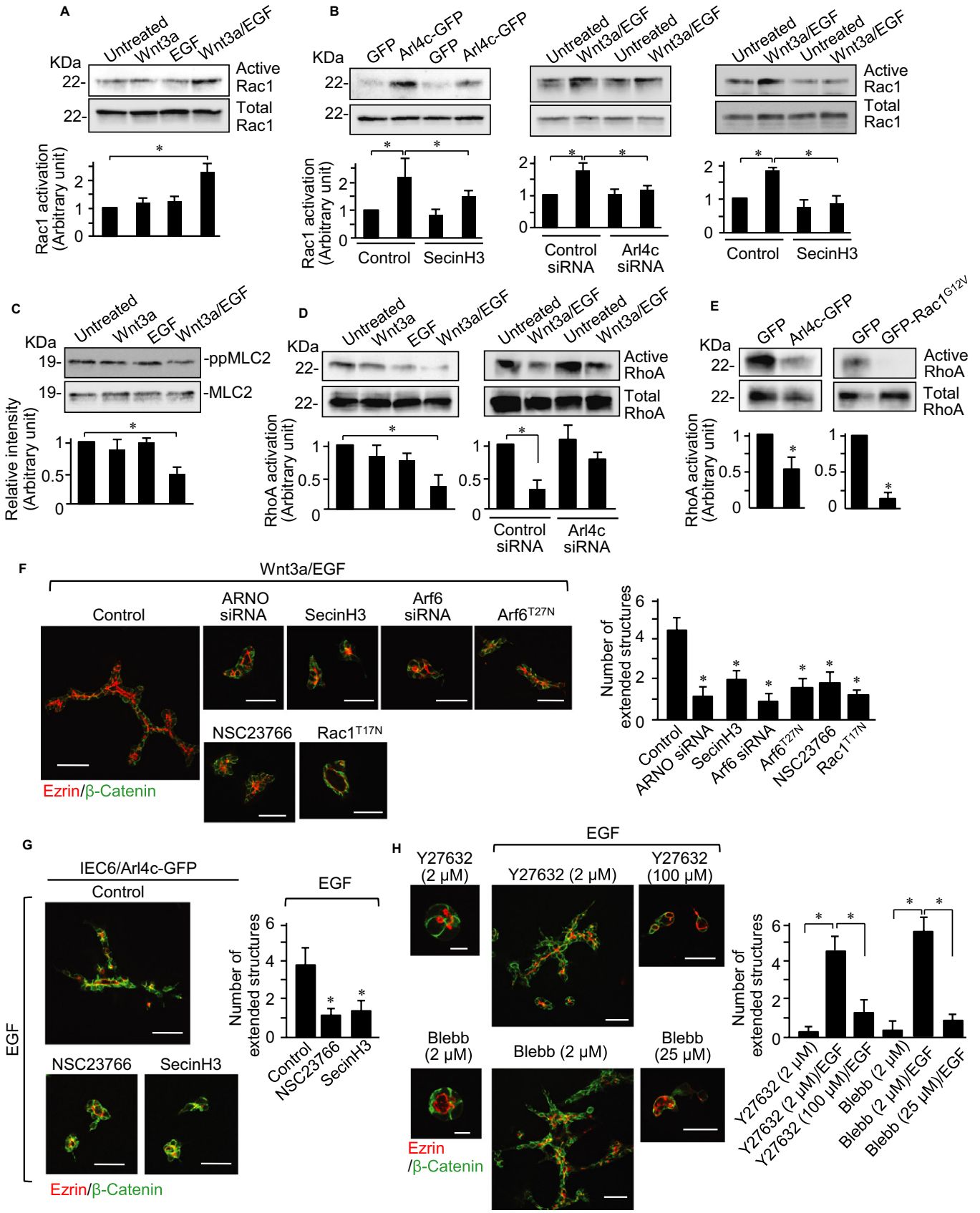

in 2D sparse culture conditions, whereas most cells had red nuclei in 2D confluent culture conditions due to contact inhibition of cell proliferation (Fig 4B). IEC6 cells in cysts in 3D culture had red nuclei, and neither EGF nor Wnt3a alone affected nuclear coloration (Fig 4B). Cells stimulated with Wnt3a/EGF had green nuclei in the extending front region of the tubes (Fig 4B). Incorporation of EdU, a marker of proliferating cells, was also observed in similar regions (Supplementary Fig S8B). These results suggest that extending cells, which express Arl4c, are growing.

Growth-arrested IEC6 cells in 3D Matrigel exhibited highly confined cell geometry at the single cell and cyst levels compared with growing and spreading cells in 2D culture (Supplementary Fig S8C). Transcription activators Yes-associated protein (YAP) and transcriptional co-activator with PDZ-binding motif (TAZ) in the Hippo pathway play a positive role in cell proliferation (Saucedo & Edgar, 2007), and ECM rigidity and cell shape influence the nuclear localization of YAP/TAZ (Dupont *et al*, 2011; Wada *et al*, 2011; Aragona *et al*, 2013). Therefore, we examined whether YAP/TAZ is involved in regulation of cell proliferation in 3D culture. Although YAP/TAZ was accumulated in the nucleus of widespread IEC6 cells grown sparsely in 2D culture, it was observed in the cytoplasm of highly confined IEC6 cells in cysts in 3D culture (Fig 4C). YAP is phosphorylated at Ser127, which induces cytoplasmic localization (Zeng & Hong, 2008), in 3D culture as well as suspension conditions, but not in 2D culture (Fig 4D). Consistent with these findings, mRNA levels of connective tissue growth factor (CTGF) and ankyrin repeat domain 1 (ANKRD1), which are target genes of YAP/TAZ, were dramatically reduced in 3D culture compared with 2D culture (Fig 4E). Treatment with Wnt3a/EGF induced nuclear localization of YAP/TAZ in the leading regions of tubes, whereas either Wnt3a or EGF alone did not (Fig 4F; Supplementary Fig S8D). Thus, Wnt3a/EGF may promote cell growth through YAP/TAZ in IEC6 cells in 3D culture.

Knockdown of Arl4c inhibited Wnt3a/EGF-induced tube formation, nuclear localization of YAP/TAZ, and nuclear incorporation of EdU (Fig 5A). YAP/TAZ was observed in the nucleus of morphologically extended IEC6 cells expressing Arl4c-GFP in the presence of EGF (Fig 5B; Supplementary Fig S8E), and Arl4c-dependent nuclear localization of YAP/TAZ was inhibited by treatment with SecinH3 or NSC23766 (Fig 5B). Treatment with Y27632/EGF or blebbistatin/EGF induced development of tubes and nuclear localization of YAP/TAZ in the extending region, although transcriptional activators were not in the nucleus following treatment with Y27632 alone (Fig 5C; Supplementary Fig S8F and G). Knockdown of YAP/TAZ inhibited Wnt3a/EGF-induced tube formation and incorporation of EdU (Fig 5D; Supplementary Fig S8H). Knockdown of YAP/TAZ also inhibited tube formation of IEC6/Arl4c-GFP cells treated with EGF (Fig 5E). These results suggest that YAP/TAZ functions downstream of Arl4c in cellular proliferation in 3D culture. Wnt3a/EGF may induce changes in cell morphology by expressing Arl4c, thereby promoting nuclear localization of YAP/TAZ, which relieves cells from immotile and less-proliferative states during tube formation.

It was recently reported that Hippo/YAP signaling crosstalks with Wnt signaling (Varelas *et al*, 2010; Heallen *et al*, 2011; Azzolin *et al*, 2012). FLAG-YAP^{5SA}, in which five possible phosphorylation Ser residues are mutated to Ala, was observed in the nucleus of IEC6 cells in 3D culture (Supplementary Fig S8I). In addition to increased CTGF mRNA levels, FLAG-YAP^{5SA} enhanced Wnt3a/EGF-induced expression of Axin2 and Arl4c mRNAs (Fig 5F). Expression of FLAG-YAP^{5SA} alone enlarged cysts and did not dramatically induce tube formation, whereas it promoted Wnt3a/EGF-induced tube formation (Fig 5G). Thus, nuclear localization of YAP/TAZ forms a positive feedback loop in Wnt3a/EGF-induced tubulogenesis by stimulating Arl4c expression.

Arl4c induces MDCK cell tube formation in 3D Matrigel culture

We examined whether Arl4c is involved in tube formation of other epithelial cell lines. Although MDCK type II (MDCK II) cells form tubes in response to HGF in 3D type I collagen gel, they did not in 3D Matrigel as shown previously (Santos & Nigam, 1993) (Fig 6A). Co-stimulation with Wnt3a and HGF or EGF did not induce tube formation, because MDCK II cells did not express Arl4c in response to Wnt3a, EGF, HGF, or their combinations (Supplementary Fig S9). However, when MDCK II cells that express Arl4c-GFP stably (MDCK/Arl4c-GFP) were stimulated with HGF, the cells extended toward the surrounding matrix and formed tubes (Fig 6A). Twenty μM Y27632 or 10 μM blebbistatin induced tube formation of MDCK II cells in the presence of HGF (Fig 6B). In addition, SecinH3 and 50 μM blebbistatin inhibited tube formation of MDCK/Arl4c-GFP cells in the presence of HGF (Fig 6C). These results suggest that changes in cell morphology through Arf6 and

Figure 3. Arl4c regulates Rac and Rho activities, inducing tube formation.

A IEC6 cells were stimulated with Wnt3a, EGF, or Wnt3a and epidermal growth factor (Wnt3a/EGF) for 18 h and subjected to the Rac assay.

B IEC6 cells expressing Arl4c-GFP were stimulated with EGF in the presence of SecinH3 (left panels) for 18 h and subjected to the Rac assay. IEC6 cells transfected with Arl4c siRNA (middle panels) or treated with SecinH3 (right panels) were stimulated with Wnt3a/EGF for 18 h and subjected to the Rac assay.

C IEC6 cells were stimulated as indicated for 18 h and whole lysates were probed with the indicated antibodies.

D IEC6 cells were stimulated as indicated for 18 h and subjected to the Rho assay (left panels). IEC6 cells transfected with Arl4c siRNA were stimulated with Wnt3a/EGF for 18 h and subjected to the Rho assay (right panels).

E IEC6 cells stably expressing GFP, Arl4c-GFP, or GFP-Rac1^{G12V} were stimulated with EGF for 18 h and subjected to the Rho assay.

F IEC6 cells transfected with Arf nucleotide-binding site opener (ARNO) or Arf6 siRNA, cells stably expressing Rac1^{T17N} or Arf6^{T27N}, and cells treated with SecinH3 or NSC23766 were stimulated with Wnt3a/EGF for 60 h in 3D culture and stained with the indicated antibodies. The number of extended structures from multicellular trunks was counted (n = 30).

G IEC6/Arl4c-GFP cells were treated with EGF in the presence or absence of NSC23766 or SecinH3 for 60 h and stained with the indicated antibodies.

H IEC6 cells were treated with Y27632 (2 μM), Y27632 (2 or 100 μM)/EGF, blebbistatin (2 μM), or blebbistatin (2 or 25 μM)/EGF for 60 h and stained with the indicated antibodies.

Data information: Results are shown as the mean ± SE from three independent experiments. Scale bars in (F and G), 50 μm; in (H), 10 μm (left two panels) and 50 μm (right four panels). *$P < 0.01$.

Source data are available online for this figure.

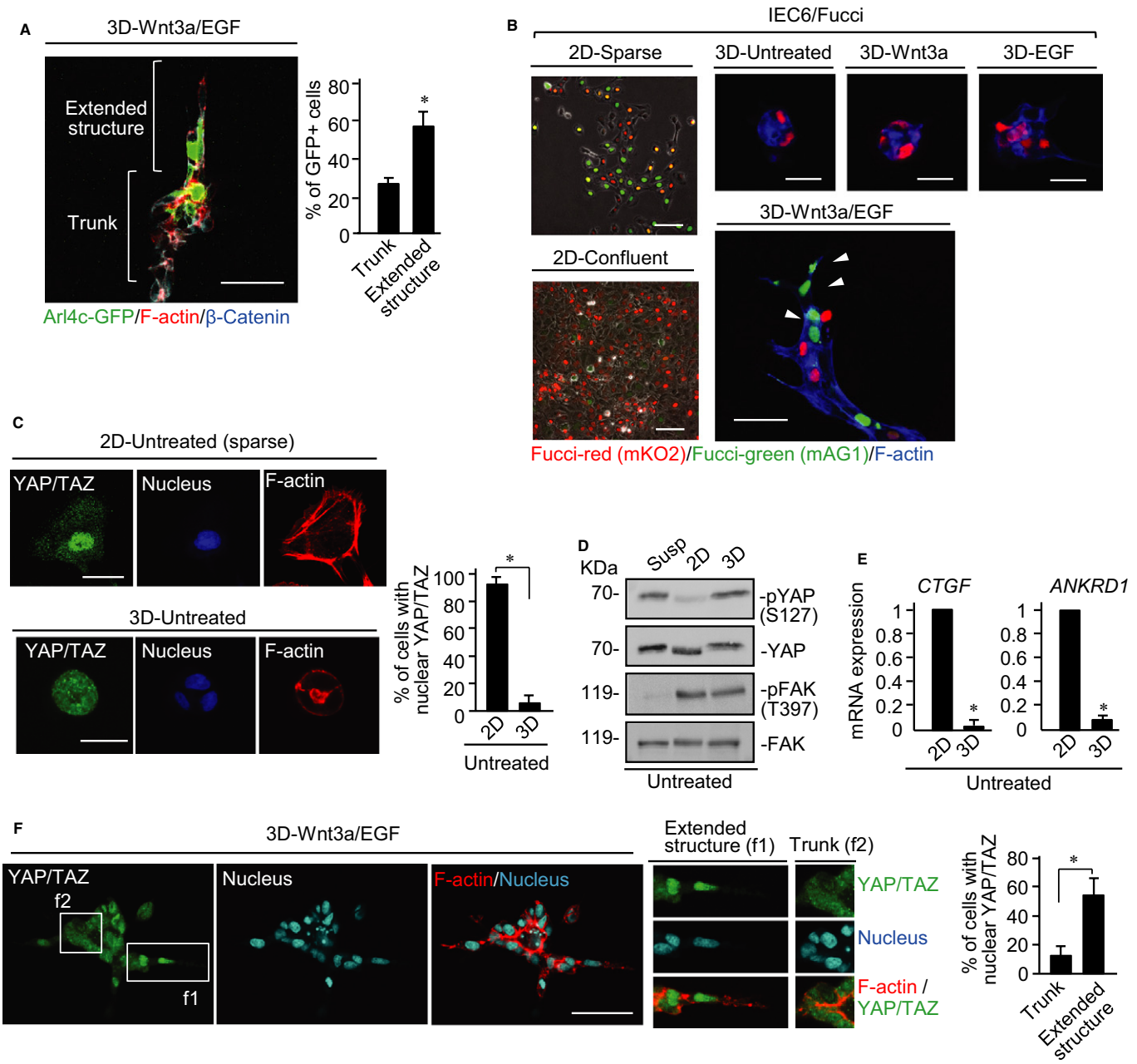

Figure 4. Wnt3a and epidermal growth factor (Wnt3a/EGF) induces nuclear localization of YAP/TAZ during tube formation.

A IEC6 cells and IEC6 cells stably expressing Arl4c-GFP were mixed at a ratio of 1:1 and treated with Wnt3a/EGF for 60 h in 3D culture. The cells were stained with the indicated antibodies and phalloidin. The number of GFP-positive cells in the extended structures and main trunks was counted (n = 40).

B IEC6 cells stably expressing the Fucci constructs were plated on a Matrigel-coated cover slip for 8 h (2D-sparse) or 60 h (2D-confluent) and photographed using phase contrast and fluorescent microscopes. IEC6/Fucci cells were cultured under the indicated conditions for 60 h in 3D Matrigel and stained with the indicated antibodies and phalloidin. White arrowheads indicate S/G2/M cells in the extending tube region.

C IEC6 cells were grown for 4 h in 2D culture or for 60 h in 3D Matrigel culture and stained with anti-YAP/TAZ antibody, DRAQ5, and phalloidin. Percentages of cells with nuclear YAP/TAZ were calculated (n = 50).

D IEC6 cells were suspended in growth medium (Susp) for 60 min, plated on 2D culture for 4 h, or seeded in 3D culture for 4 h. Lysates were probed with anti-phospho YAP (Ser127), anti-YAP, anti-phospho FAK (Tyr397), and anti-FAK antibodies.

E IEC6 cells were cultured for 3 h in 2D or 3D culture and *CTGF* and *ANKRD1* mRNA levels were measured.

F IEC6 cells were treated with Wnt3a/EGF for 48 h and then stained with anti-YAP/TAZ antibody, DRAQ5, and phalloidin. White boxes show enlarged images. Percentages of cells with nuclear YAP/TAZ were calculated (n = 50).

Data information: Results are shown as the means ± SE from three independent experiments. Scale bars in (A and F), 50 μm; in (B), 100 μm (left two panels), 20 μm (upper right three panels), and 50 μm (lower right panel); in (C), 20 μm. *P < 0.01.

Source data are available online for this figure.

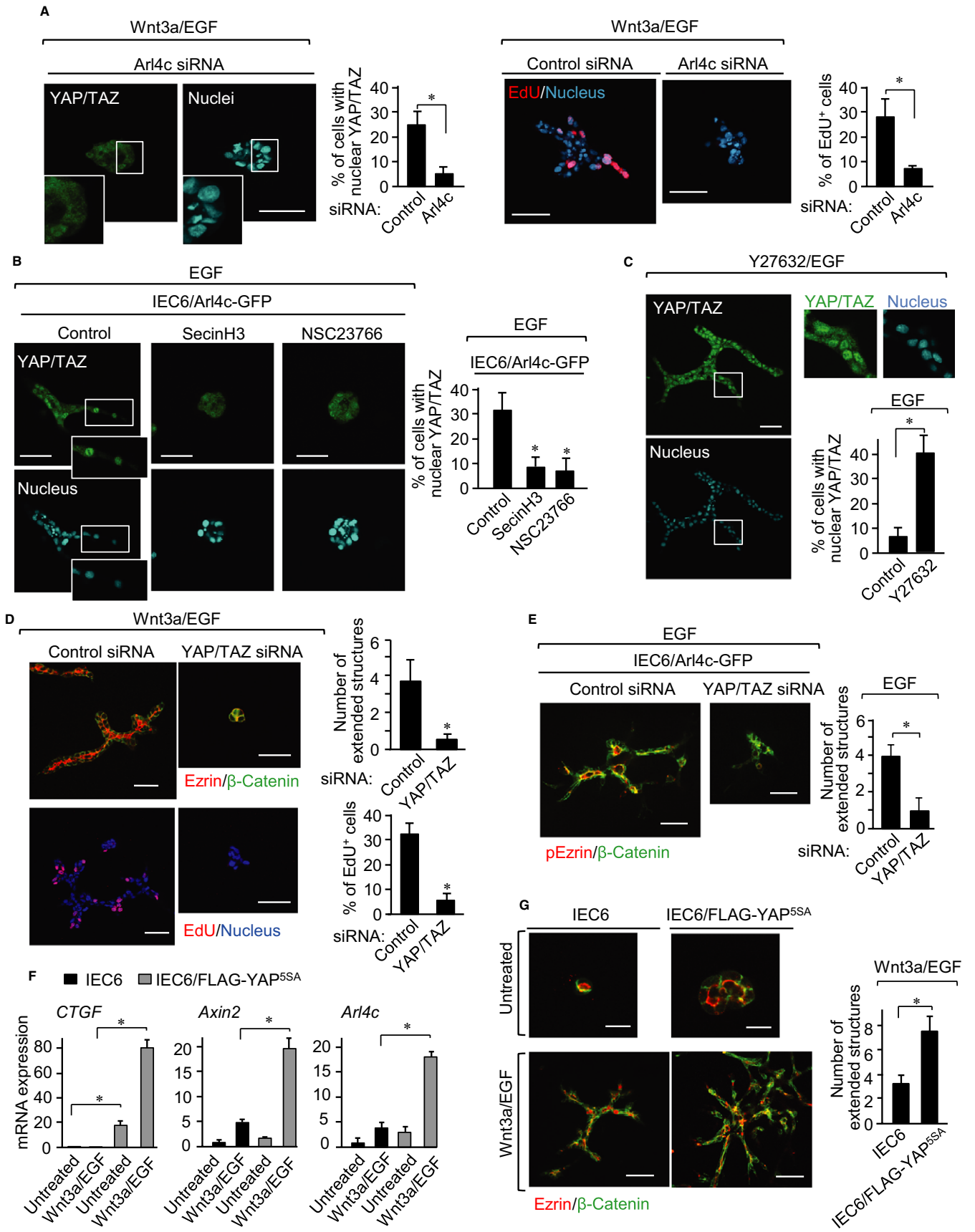
A
Wnt3a/EGF
Arl4c siRNA
YAP/TAZ
Nuclei
% of cells with nuclear YAP/TAZ
siRNA: Control Arl4c
Wnt3a/EGF
Control siRNA
Arl4c siRNA
EdU/Nucleus
% of EdU+ cells
siRNA: Control Arl4c
B
EGF
IEC6/Arl4c-GFP
Control
SecinH3
NSC23766
YAP/TAZ
Nucleus
% of cells with nuclear YAP/TAZ
Control SecinH3 NSC23766
C
Y27632/EGF
YAP/TAZ
Nucleus
EGF
% of cells with nuclear YAP/TAZ
Control Y27632
D
Wnt3a/EGF
Control siRNA
YAP/TAZ siRNA
Ezrin/β-Catenin
EdU/Nucleus
Number of extended structures
% of EdU+ cells
siRNA: Control YAP/TAZ
E
EGF
IEC6/Arl4c-GFP
Control siRNA
YAP/TAZ siRNA
pEzrin/β-Catenin
Number of extended structures
siRNA: Control YAP/TAZ
F
IEC6
IEC6/FLAG-YAP5SA
CTGF
Axin2
Arl4c
mRNA expression
Untreated Wnt3a/EGF Untreated Wnt3a/EGF
G
IEC6
IEC6/FLAG-YAP5SA
Untreated
Wnt3a/EGF
Ezrin/β-Catenin
Wnt3a/EGF
Number of extended structures
IEC6
IEC6/FLAG-YAP5SA

Rho contribute to induce development of tubes by MDCK II cells as well as IEC6 cells.

Arl4c is involved in branching morphogenesis in mouse embryonic kidneys

We evaluated the involvement of Arl4c in tubular organ development. Arl4c mRNA levels were relatively high in the mouse kidneys, brain, submandibular glands (SMGs), lungs, stomach, and intestines at embryonic day 13 (E13) (Supplementary Fig S10A). Immunohistochemical analyses revealed that Arl4c is expressed in the brain and some epithelial rudiments, including hair follicle, tooth bud, salivary gland, and kidney, of E15 mouse embryos (Supplementary Fig S10B). In the embryonic kidney, Arl4c was observed in UBs, pretubular aggregates, renal vesicles, and the comma-shaped body (Fig 7A). Arl4c was particularly localized to UB tips in pan-cytokeratin staining regions and expressed in neural cell adhesion molecule (NCAM)-staining regions (Fig 7A). Pan-cytokeratin is an ureteric cell marker (Song *et al*, 2010), and NCAM is a marker for induced mesenchyme (Marciano *et al*, 2011).

Arl4c mRNA was expressed more abundantly in the epithelium than the mesenchyme of kidney rudiments at E12 (Supplementary Fig S10C). Kidney rudiments induced elongation of the collecting ducts and increased the number and size of nephrons after 72 h (Hendry *et al*, 2011; Zhang *et al*, 2012) (Fig 7B). Arl4c mRNA levels increased during this process but were reduced by treatment of the rudiments with IWP2, which inhibited Wnt secretion (Chen *et al*, 2009) (Fig 7B), suggesting that endogenous Wnt is involved in Arl4c expression in the developing kidney. In contrast, CHIR99021 increased Arl4c mRNA expression (Fig 7B). Treatment of the rudiments with U0126 or IWP2/U0126 inhibited upregulation of Arl4c mRNA levels to the same extent as FIIN-1, an inhibitor of receptor for fibroblast growth factor (FGF) (Fig 7B). FGF is released from the mesenchyme and is essential for kidney development (Qiao *et al*, 2001; Bates, 2011). SecinH3 and NSC23766 did not affect Arl4c expression (Fig 7B), confirming that Arf6 and Rac function downstream of Arl4c. Consistent with previous observations that the MEK inhibitor PD98059 inhibits UB branching of kidney organs (Watanabe & Costantini, 2004), U0126 also reduced the number of UB tips (Fig 7C). IWP2, SecinH3, and NSC23766 showed similar effects, and the combination of IWP2 and U0126 inhibited branching morphogenesis to a similar extent as FIIN-1 (Fig 7C). Active caspase-3-positive cells were observed in the interior of ureteric ducts and the mesenchyme region, but only a few cell died at UB tips (Supplementary Fig S10D). Treatment with IWP2, U0126, IWP2/U0126, and FIIN-1 did not increase cell death at UB tips, suggesting that these inhibitors do not affect viability of UB epithelial cells.

It has been shown that mesenchyme-free UBs undergo repetitive rounds of cleft and bud formation to form branched epithelial organoids in the presence of FGF and conditioned medium from metanephric mesenchymal cells (Sakurai *et al*, 1997; Qiao *et al*, 1999, 2001). We developed a system in which UBs undergo branching morphogenesis in medium containing FGF1, glial cell line-derived neurotrophic factor (GDNF), and R-spondin1 without conditioned medium (Fig 7D). GDNF is released from the cap mesenchyme and is necessary for early UB outgrowth (Qiao *et al*, 1999). R-spondin1 enhances β-catenin-dependent Wnt signaling by binding to Lgr5 homologs (de Lau *et al*, 2011). All of FGF1, GDNF, and R-spondin1 were required for efficient UB growth (Supplementary Fig S11A). In addition, nuclear localization of YAP/TAZ was observed in cells in buds but not trunks, and Ki67-positive cells were also detected in buds more abundantly than in trunks (Supplementary Fig S11B). These results indicate that cells tend to proliferate at UB tips. IWP2, U0126, NSC23766, or SecinH3 decreased bud numbers of organoids (Fig 7E). In contrast, CHIR99021 or 20 μM Y27632 did not affect bud numbers but increased the size of branched structures due to enlargement of the epithelial bud (Fig 7E). In addition, knockdown of Arl4c inhibited bud formation of organoids (Fig 7F). Consistent with findings in IEC6 cells, Wnt may induce Arl4c expression in concert with growth factors, such as FGF, resulting in formation of epithelial tubes in the embryonic kidney through regulation of Arf6, Rac, and Rho.

Discussion

We used IEC6 cells as a model to analyze epithelial tube formation in 3D BMM culture and identified an Arl4c signaling mechanism that regulates tubulogenesis. This model suggests that the Wnt-β-catenin and EGF-MAPK pathways work in concert to induce Arl4c expression, resulting in changes in cell morphology and cell proliferation to form epithelial tubes (Supplementary Fig S12). In cooperation with EGF signaling, stabilization of β-catenin by Wnt3a signaling enhanced formation of a complex between Tcf4, Ets, and CBP

Figure 5. Arl4c and YAP/TAZ mutually regulate their expression and functions.

A IEC6 cells transfected with Arl4c siRNA were treated with Wnt3a and epidermal growth factor (Wnt3a/EGF) for 60 h in 3D culture and stained with anti-YAP/TAZ antibody, DRAQ5, and phalloidin (left panels). The cells were also incubated with EdU for 20 min before fixation and stained with DRAQ5 (right panels). White boxes show enlarged images. Percentages of cells with nuclear YAP/TAZ (left panels) and EdU-positive cells (right panels) were calculated (n = 50).

B IEC6/Arl4c-GFP cells were treated with EGF in the presence or absence of SecinH3 or NSC23766 for 48 h and stained with the indicated antibodies.

C IEC6 cells were treated with Y27632 (2 μM)/EGF for 60 h and stained with anti-YAP/TAZ antibody, DRAQ5, and phalloidin.

D IEC6 cells transfected with YAP/TAZ siRNA were treated with Wnt3a/EGF for 60 h and stained with the indicated antibodies, or the cells were incubated with EdU for 20 min before fixation and stained with DRAQ5. The number of extended structures from multicellular trunks (n = 30) and percentages of EdU-positive cells (n = 50) were calculated.

E IEC6/Arl4c-GFP cells transfected with YAP/TAZ siRNA were treated with EGF for 60 h and stained with the indicated antibodies.

F IEC6 cells or IEC6 cells stably expressing FLAG-YAP^{5SA} (IEC6/FLAG-YAP^{5SA}) were cultured with or without Wnt3a/EGF for 5 h in 3D culture to measure *CTGF*, *Axin2*, and *Arl4c* mRNA levels.

G IEC6 cells or IEC6/FLAG-YAP^{5SA} cells were treated with Wnt3a/EGF for 60 h and stained with the indicated antibodies.

Data information: Results are shown as the mean ± SE from three independent experiments. Scale bars in (A-E), 50 μm; in (G), 20 μm (top panels) and 50 μm (bottom panels). *$P < 0.01$.

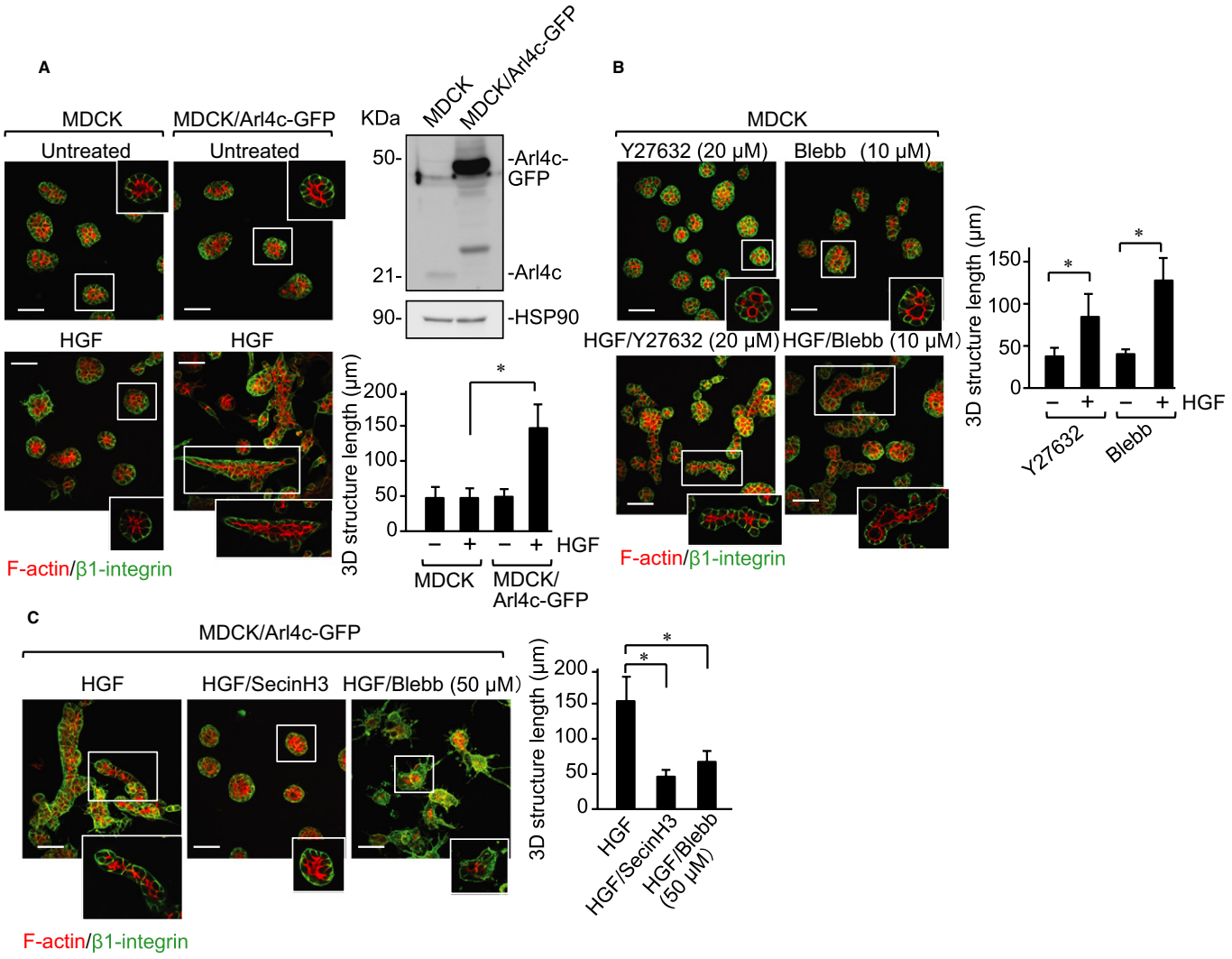

Figure 6. Arl4c is involved in hepatocyte growth factor (HGF)-dependent branching morphogenesis of Madin Darby canine kidney (MDCK) II cells in 3D Matrigel.

A MDCK II cells or MDCK II cells stably expressing Arl4c-GFP (MDCK/Arl4c-GFP) were treated with or without HGF for 60 h in 3D culture. The cells were stained with anti-β1-integrin antibody and phalloidin (stacking image). Whole lysates were probed with anti-Arl4c and anti-HSP90 antibodies. The longest length of tube-like structures was measured (n = 30). The middle sections of white boxes are shown in the corner of each picture.

B MDCK II cells were treated with Y27632 (20 μM), Y27632 (20 μM)/HGF, blebbistatin (10 μM), or blebbistatin (10 μM)/HGF for 60 h and stained with anti-β1-integrin antibody and phalloidin (stacking image).

C MDCK/Arl4c-GFP cells were treated with HGF, HGF/SecinH3, or HGF/blebbistatin (50 μM) for 60 h and stained with anti-β1-integrin antibody and phalloidin (stacking image).

Data information: Results are shown as the mean ± SE from three independent experiments. Scale bars in (A–C), 50 μm. *P < 0.01.

Source data are available online for this figure.

on the Ets-binding site in the 3′-UTR of the *Arl4c* gene, thereby inducing Arl4c expression. The Tcf/LEF-binding-site on the *Arl4c* gene has not yet been identified. It is also possible that Wnt3a and EGF activate Tcf4 and Ets, which bind to the different regions of the *Arl4c* gene to induce its expression. In 3D culture, epithelial cells are compact, immotile, and less proliferative. To form tubes in 3D conditions, epithelial cells have to be partially depolarized, motile, mitotic, and finally re-polarized. Therefore, actomyosin rearrangement by Rac and Rho, of which activities are regulated by Arl4c expression, is important for tube formation of IEC6 cells. However, expression of Arl4c alone or treatment with Y27632 or blebbistatin alone was not sufficient for tube formation, and EGF signaling was required to induce tube formation. In addition to signals to regulate the cytoskeleton properly, cell growth signals are necessary for tubulogenesis.

Arl4c expression by Wnt3a/EGF in IEC6 cells activated Rac1 through ARNO and Arf6, resulting in proper inhibition of RhoA, during tube formation. We showed that HGF does not affect cyst morphology of MDCK II cells in 3D Matrigel but develops tube formation when Arl4c is expressed. The combination of HGF and

Y27632 or blebbistatin induced wild-type MDCK II cell tube formation and SecinH3 inhibited HGF-induced tube development of MDCK/Arl4c-GFP cells. It was reported that unlike MDCK II cells, HGF induces tubes from MDCK type I cells in 3D Matrigel (Tushir & D'Souza-Schorey, 2007). In this model, HGF-induced Arf6 activation promotes the recruitment of Rac1 to the cell surface at the initiation of tube formation. Further, Arf6 activation also upregulates MAPK activity and the expression of the urokinase-type plasminogen activator receptor, which induces Rac1 activation probably through the DOCK180/Elmo complex, a Rac1 activator. Therefore, a cellular apparatus downstream of Arf6 activation, including the Rac and Rho axis, might be common in tube formation of IEC6 and MDCK I and II cells.

Our model in cultured epithelial cells is applicable to an organ culture model using the mouse embryonic kidney. Arl4c mRNA, which is primarily expressed in the epithelium, increased during epithelial tube elongation and branching of kidney rudiments. Wnt or MAPK signaling was required for Arl4c expression, and simultaneous inhibition of both pathways inhibited kidney development to a similar extent to inhibition of FGF signaling. We established a system in which FGF1, GDNF, and R-spondin1 induce branching morphogenesis in UBs in 3D Matrigel. In this culture, activation of β-catenin signaling or proper inhibition of Rho signaling enhanced organoid development, while inhibition of MAPK, ARNO, and Rac suppressed it. Conditioned medium from the metanephric mesenchyme (BSN-CM) and a mixture of growth factors (GDNF and FGF1) are required for branching morphogenesis of UBs *in vitro* (Qiao *et al*, 1999). Because our system does not include BSN-CM, it would be useful to define the soluble factors required for branching within UB. The β-catenin-dependent pathway regulates branching and maintains UB cells in an undifferentiated state (Bridgewater *et al*, 2008; Marose *et al*, 2008). However, the Wnt ligand that mediates the β-catenin-dependent pathway remains to be elucidated. The Wnt ligand expressed by UBs could act in an autocrine manner, because R-spondin1 is required in our culture system. Results from different systems suggest that changes in cell morphology by proper actomyosin rearrangement through Arl4c expression are linked to the formation of tubular structures.

Tubulogenesis involves cell proliferation. Although it has been shown that cell division is required for tube formation (Yu *et al*, 2003), how epithelial morphological changes influences cell proliferation is not known. Proliferating cells in the extending tubes of IEC6 cells and buds of kidney organoids showed nuclear localization of YAP/TAZ. However, nuclear localization of YAP/TAZ was not sufficient for tube formation of IEC6 cells, although cysts were enlarged. YAP/TAZ expression enhanced Wnt3a/EGF-induced tube formation, suggesting that cytoskeletal changes would promote cell proliferation dramatically for tubulogenesis under physiological conditions. Several studies have shown bidirectional crosstalk between Hippo and Wnt/β-catenin signaling through direct interaction of YAP/TAZ with Dvl or β-catenin, depending on the biological context (Varelas *et al*, 2010; Heallen *et al*, 2011; Azzolin *et al*, 2012; Bernascone & Martin-Belmonte, 2013). Our results showed that Wnt3a/EGF signaling induces nuclear translocation of YAP/TAZ through Arl4c expression in the front region of extending tubes and that YAP enhances Wnt3a/EGF-induced Arl4c expression, suggesting a positive feedback loop between Hippo, Wnt, and growth factors signaling. Thus, mutual regulation between cell proliferation and cytoskeletal rearrangement by Wnt and growth factors is essential for tubulogenesis of epithelial cells. It was shown that changes in cell shape are conserved cellular events during tube formation and that cell proliferation is also necessary for it (Yu *et al*, 2003; Lu & Werb, 2008). Contact between mammary epithelial cells and type I collagen in the ECM caused traction force to extend and stabilize linear patterns of tubes (Guo *et al*, 2012). In addition, mechanical stress induced by ECM stiffness and cytoskeletal tension controlled epithelial multicellular growth by regulating YAP/TAZ nuclear localization (Aragona *et al*, 2013). Thus, YAP/TAZ likely connects these cellular events during tubulogenesis.

Materials and Methods

3D culture of IEC6 and MDCK II cells

To analyze 3D epithelial morphogenesis in Matrigel (BD Biosciences, San Jose, CA, USA), 40 μl of Matrigel was mounted on a round coverslip and incubated for 30 min at 37°C to solidify the gel. IEC6 cells (4×10^4 cells) suspended in 1 ml of growth medium containing 2% Matrigel (V/V), 40 ng/ml Wnt3a, and/or 5 ng/ml EGF (R&D Systems, Minneapolis, MN, USA) were added on solid Matrigel and incubated for 72 h. When necessary, 50 ng/ml Wnt5a, 10 ng/ml HGF (R&D), 10 μM IWR1, 5 μM CHIR99021, 100 μM NSC23766, 2 or 25 μM blebbistatin, 2 or 100 μM Y27632, or 25 μM SecinH3, were

Figure 7. Arl4c is involved in branching morphogenesis in the mouse embryonic kidney.

A Tissue sections of mouse kidney at embryonic day 15 (E15) were stained with anti-Arl4c antibody and hematoxylin (left panels). Sections were also stained with anti-Arl4c, anti-neural cell adhesion molecule (NCAM), and anti-pan-cytokeratin antibodies and DRAQ5 (right panels). Black and white boxes show enlarged images.

B Kidney rudiments at E12 were cultured on transwell filters with or without the indicated reagents for 72 h, and real-time PCR analyses for *Arl4c* mRNA expression were performed.

C Kidney rudiments at E12 were cultured on transwell filters with or without the indicated reagents for 48 h and stained with an anti-cytokeratin8 antibody. The number of UB tips was counted ($n = 5$).

D Ureteric buds isolated from E12 mouse kidneys were cultured with fibroblast growth factor 1 (FGF1), glial cell line-derived neurotrophic factor (GDNF), and R-spomdin1 for 7 days in 3D Matrigel.

E UBs isolated from E12 mouse kidneys were cultured in 3D Matrigel with or without the indicated reagents for 7 days and stained with phalloidin and DRAQ5 (stacking image). White boxes show enlarged pictures. The number of epithelial buds was counted ($n = 5$). The area of the control, CHIR99021-, or Y27632-treated organoids was measured ($n = 5$).

F UBs infected with lentiviruses containing control or Arl4c shRNA were cultured in 3D Matrigel for 7 days and stained with anti-E-cadherin and phalloidin (stacking image). White boxes show enlarged images. Real-time PCR analyses for *Arl4c* mRNA expression were performed. Results are shown as the mean ± SE from three independent experiments. Scale bars in (A), 250 μm (upper left panel) and 300 μm (upper right two panels); in (B and C), 500 μm; in (D), 250 μm; in (E and F), 200 μm. *$P < 0.01$.

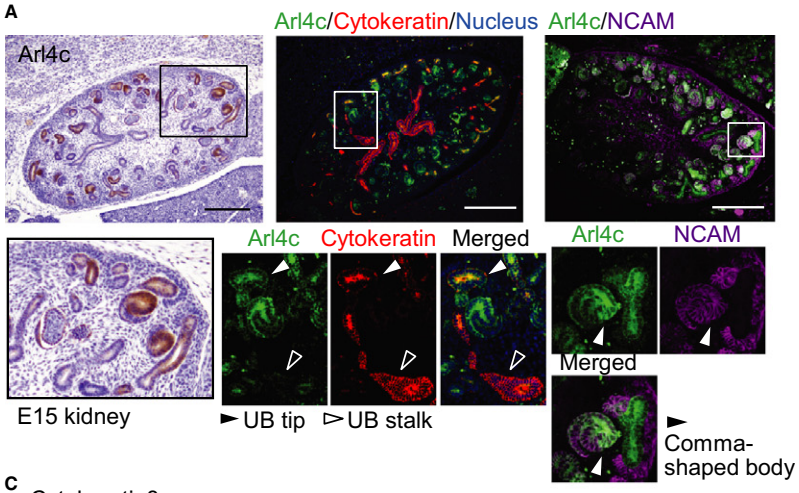

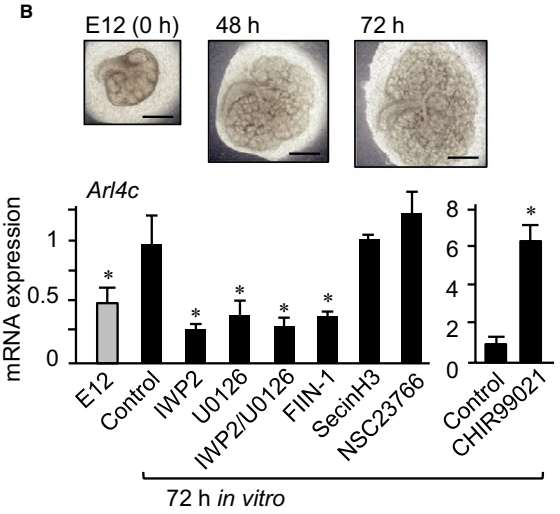

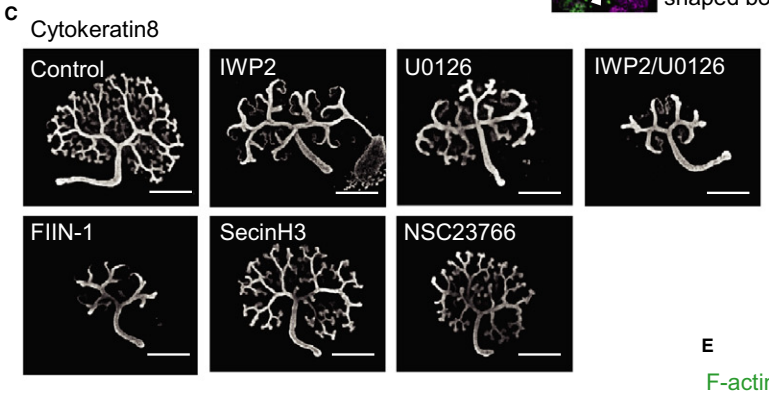

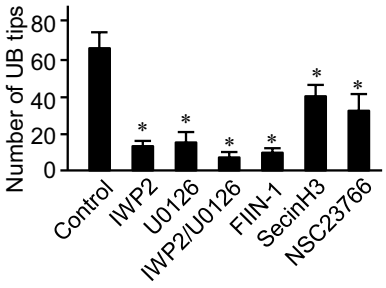

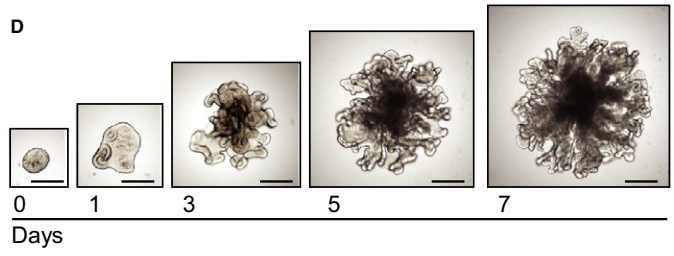

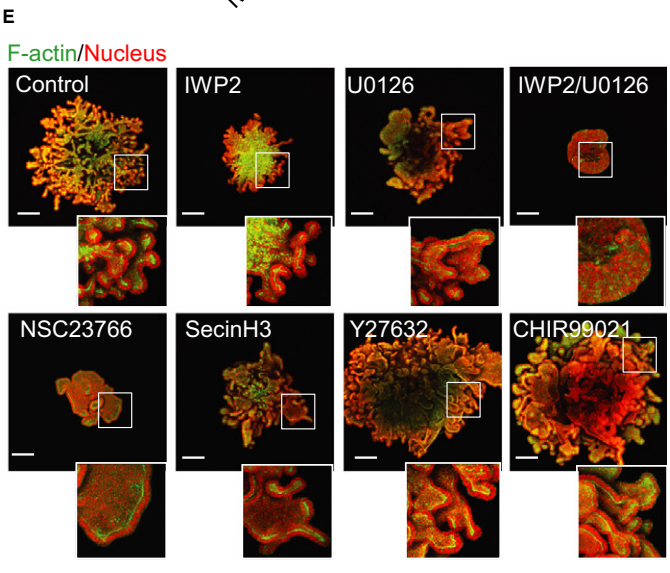

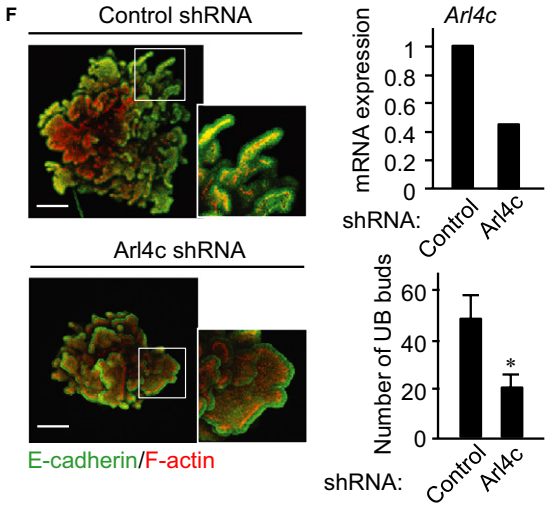

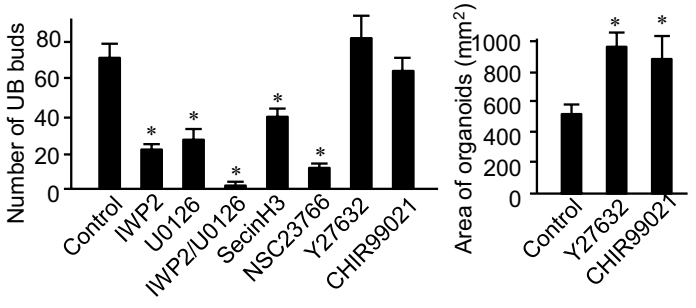

added to the growth medium. The extended structure was defined as a chain- or cord-like structure containing at least four cells that extended from the main multicellular trunks. The number of extended structures from multicellular trunks was counted.

MDCK type II (MDCK II) cells were used in this study. MDCK II cells expressing Arl4c were three-dimensionally cultured under the same conditions as IEC6 cells in the presence of 20 ng/ml HGF, 20 μM Y27632, 10 or 50 μM blebbistatin, and/or 25 μM SecinH3. The length of tube-like structures was measured.

2D culture on Matrigel-coated dishes

Glass coverslips were coated with Matrigel. IEC6 cells were grown on a Matrigel-coated dish in α minimum essential medium (MEM) containing 10% fetal calf serum (FCS) and treated with 40 ng/ml Wnt3a, 5 ng/ml EGF, 100 μM NSC23766, 25 μM SecinH3, 2 μM blebbistatin, 2 μM Y27632, or 10 μM actinomycin D.

Organ and organoid kidney culture

Embryonic kidneys isolated from E12 mice (C57BL/6J) were cultured in an air–liquid interface on Transwell culture inserts with 1-μm pores (Greiner Bio-One SAS, Courtaboeuf, France) in DMEM/Ham's F12 supplemented with 10% FCS and penicillin-streptomycin. The number of UB tips was counted as described (Li *et al*, 2005).

For organoid culture, E12 embryonic kidneys were treated with dispase, separated into UBs and metanephric mesenchyme using a fine tungsten needle, and collected in 10% BSA/DMEM/Ham's F12. After isolated UB were placed in 30 μl of Matrigel and incubated for 30 min at 37°C to solidify the gel, UBs were grown in αMEM supplemented with penicillin-streptomycin, 4.5 mg/ml glucose, 10 μg/ml insulin, and 1× non-essential amino acids, 10 mM HEPES, Glutamax, 1× N2, 1× B27, 1 mM N-acetylcysteine, 200 ng/ml FGF1, 100 ng/ml GDNF (R&D), 200 ng/ml R-spondin1 (R&D), and 10% FCS for 7 days. When necessary, 5 μM IWP2, 1 μM (UB organoid culture) or 5 μM (kidney organ culture) CHIR99021, 10 μM U0126, 500 nM FIIN-1, 25 μM (kidney organ culture) or 100 μM (UB organoid culture) NSC23766, 25 μM SecinH3, or 20 μM Y27632 were added to the same growth medium. The number of epithelial buds was counted, and the area of individual organoids was measured using a LSM image browser (Carl-Zeiss, Jena, Germany).

Immunohistochemical evaluation of Arl4c in mouse embryos

Embryos derived from C57BL/6J mice at embryonic day 15 (E15) were dissected in PBS and fixed for 1 h in PBS containing 4% (w/v) PFA. Paraffin-embedded samples of mouse embryos were sectioned. Antigen retrieval with a Pascal pressurized heating chamber (Dako, Carpinteria, CA, USA) was conducted for staining. For immunostaining of Arl4c, a Dako ENVISION kit (Dako) was used in accordance with the manufacturer's recommendations. Anti-Arl4c antibody was incubated with tissue samples overnight at 4°C and detected by incubation with goat anti-rabbit IgG-horseradish peroxidase (HRP). The signal was visualized using a substrate-chromogen solution. The sections were counterstained with 0.1% hematoxylin. For immunofluorescence staining of Arl4c, antigen-retrieved tissue sections were blocked in PBS containing 0.5% (w/v) Triton X-100 and 40 mg/ml BSA for 30 min and incubated with primary antibodies for 3 h at room temperature and secondary antibodies in accordance with the manufacturer's protocol (Life Technologies, Carlsbad, CA, USA).

Statistical analyses

The experiments were repeated three or four times, and the results were expressed as means ± SE. Statistical analyses were performed using StatView software (SAS Institute Inc.). Differences between the data were tested for statistical significance using *t*-test. *P*-values less than 0.01 were considered statistically significant.

Supplementary information for this article is available online: http://emboj.embopress.org

Acknowledgements

We thank Drs. H. Shiratori, H. Hamada, R. Nishinakamura, and T. Kurimoto for valuable discussion regarding Arl4c expression and technical assistance. We also thank Drs. A. Miyawaki, H. Miyoshi, K. Nakayama, and C. Marshall for donating plasmids and RIKEN BRC for providing the B6N mouse BAC clone. This work was supported by Grants-in-Aid for Scientific Research to A.K. (2009–2011) (No. 21249017) and S.M. (2011–2013) (No. 23790333) and for Scientific Research on Innovative Areas to A.K. (2011–2013) (No. 23112004) from the Ministry of Education, Science, and Culture of Japan.

Author contributions

SM designed experiments, performed cellular and organ culture experiments, and wrote the manuscript. SF and AS performed cellular experiments and SI performed organ culture experiments. MI and YK generated lentivirus harvoring a Fucci construcut and provided advice. AK designed experiments and wrote the manuscript.

Conflict of interest

The authors declare that they have no conflict of interest.

References

van Amerongen R, Berns A (2006) Knockout mouse models to study Wnt signal transduction. *Trends Genet* 22: 678–689

Aragona M, Panciera T, Manfirin A, Giulitti S, Michielin F, Elvassore N, Dupont S, Piccolo S (2013) A mechanical checkpoint controls multicellular growth through YAP/TAZ regulation by actin-processing factors. *Cell* 154: 1047–1059

Avraham R, Yarden Y (2011) Feedback regulation of EGFR signalling: decision making by early and delayed loops. *Nat Rev Mol Cell Biol* 12: 104–117

Azzolin L, Zanconato F, Bresolin S, Forcato M, Basso G, Bicciato S, Cordenonsi M, Piccolo S (2012) Role of TAZ as Mediator of Wnt Signaling. *Cell* 151: 1443–1456

Bates CM (2011) Role of fibroblast growth factor receptor signaling in kidney development. *Am J Physiol Renal Physiol* 301: F245–F251

Bernascone I, Martin-Belmonte F (2013) Crossroads of Wnt and Hippo in epithelial tissues. *Trends Cell Biol* 23: 380–389

Bridgewater D, Cox B, Cain J, Lau A, Athaide V, Gill PS, Kuure S, Sainio K, Rosenblum ND (2008) Canonical WNT/β-catenin signaling is required for ureteric branching. *Dev Biol* 317: 83–94

Bryant DM, Mostov KE (2008) From cells to organs: building polarized tissue. *Nat Rev Mol Cell Biol* 9: 887–901

Burd CG, Strochlic TI, Gangi Setty SR (2004) Arf-like GTPases: not so Arf-like after all. *Trends Cell Biol* 14: 687–694

Chen B, Dodge ME, Tang W, Lu J, Ma Z, Fan CW, Wei S, Hao W, Kilgore J, Williams NS, Roth MG, Amatruda JF, Chen C, Lum L (2009) Small molecule-mediated disruption of Wnt-dependent signaling in tissue regeneration and cancer. *Nat Chem Biol* 5: 100–107

Debnath J, Brugge JS (2005) Modelling glandular epithelial cancers in three-dimensional cultures. *Nat Rev Cancer* 5: 675–688

Debnath J, Mills KR, Collins NL, Reginato MJ, Muthuswamy SK, Brugge JS (2002) The role of apoptosis in creating and maintaining luminal space within normal and oncogene-expressing mammary acini. *Cell* 111: 29–40

Dupont S, Morsut L, Aragona M, Enzo E, Giulitti S, Cordenonsi M, Zanconato F, Le Digabel J, Forcato M, Bicciato S, Elvassore N, Piccolo S (2011) Role of YAP/TAZ in mechanotransduction. *Nature* 474: 179–183

Gao Y, Dickerson JB, Guo F, Zheng J, Zheng Y (2004) Rational design and characterization of a Rac GTPase-specific small molecule inhibitor. *Proc Natl Acad Sci USA* 101: 7618–7623

Garrett-Sinha LA (2013) Review of Ets1 structure, function, and roles in immunity. *Cell Mol Life Sci* 70: 3375–3390

Gon H, Fumoto K, Ku Y, Matsumoto S, Kikuchi A (2013) Wnt5a signaling promotes apical and basolateral polarization of single epithelial cells. *Mol Biol Cell* 23: 3764–3774

Gumbiner BM (1992) Epithelial morphogenesis. *Cell* 69: 385–387

Guo CL, Ouyang M, Yu JY, Maslov J, Price A, Shen CY (2012) Long-range mechanical force enables self-assembly of epithelial tubular patterns. *Proc Natl Acad Sci USA* 109: 5576–5582

Hafner M, Schmitz A, Grune I, Srivatsan SG, Paul B, Kolanus W, Quast T, Kremmer E, Bauer I, Famulok M (2006) Inhibition of cytohesins by SecinH3 leads to hepatic insulin resistance. *Nature* 444: 941–944

Heallen T, Zhang M, Wang J, Bonilla-Claudio M, Klysik E, Johnson RL, Martin JF (2011) Hippo pathway inhibits Wnt signaling to restrain cardiomyocyte proliferation and heart size. *Science* 332: 458–461

Hendry C, Rumballe B, Moritz K, Little MH (2011) Defining and redefining the nephron progenitor population. *Pediatr Nephrol* 26: 1395–1406

Hoffman MP, Kibbey MC, Letterio JJ, Kleinman HK (1996) Role of laminin-1 and TGF-β3 in acinar differentiation of a human submandibular gland cell line (HSG). *J Cell Sci* 109: 2013–2021

Hofmann I, Thompson A, Sanderson CM, Munro S (2007) The Arl4 family of small G proteins can recruit the cytohesin Arf6 exchange factors to the plasma membrane. *Curr Biol* 17: 711–716

Kikuchi A, Yamamoto H, Sato A, Matsumoto S (2011) New insights into the mechanism of wnt signaling pathway activation. *Int Rev Cell Mol Biol* 291: 21–71

Koo TH, Eipper BA, Donaldson JG (2007) Arf6 recruits the Rac GEF Kalirin to the plasma membrane facilitating Rac activation. *BMC Cell Biol* 8: 29

Korff T, Augustin HG (1998) Integration of endothelial cells in multicellular spheroids prevents apoptosis and induces differentiation. *J Cell Biol* 143: 1341–1352

de Lau W, Barker N, Low TY, Koo BK, Li VS, Teunissen H, Kujala P, Haegebarth A, Peters PJ, van de Wetering M, Stange DE, van Es JE, Guardavaccaro D, Schasfoort RB, Mohri Y, Nishimori K, Mohammed S, Heck AJ, Clevers H (2011) Lgr5 homologues associate with Wnt receptors and mediate R-spondin signalling. *Nature* 476: 293–297

Li X, Hyink DP, Polgar K, Gusella GL, Wilson PD, Burrow CR (2005) Protein kinase X activates ureteric bud branching morphogenesis in developing mouse metanephric kidney. *J Am Soc Nephrol* 16: 3543–3552

Lu P, Werb Z (2008) Patterning mechanisms of branched organs. *Science* 322: 1506–1509

Marciano DK, Brakeman PR, Lee CZ, Spivak N, Eastburn DJ, Bryant DM, Beaudoin GM 3rd, Hofmann I, Mostov KE, Reichardt LF (2011) p120 catenin is required for normal renal tubulogenesis and glomerulogenesis. *Development* 138: 2099–2109

Marose TD, Merkel CE, McMahon AP, Carroll TJ (2008) β-Catenin is necessary to keep cells of ureteric bud/Wolffian duct epithelium in a precursor state. *Dev Biol* 314: 112–126

Miller RK, McCrea PD (2010) Wnt to build a tube: contributions of Wnt signaling to epithelial tubulogenesis. *Dev Dyn* 239: 77–93

O'Brien LE, Zegers MM, Mostov KE (2002) Opinion: building epithelial architecture: insights from three-dimensional culture models. *Nat Rev Mol Cell Biol* 3: 531–537

Ohtsuka N, Urase K, Momoi T, Nogawa H (2001) Induction of bud formation of embryonic mouse tracheal epithelium by fibroblast growth factor plus transferrin in mesenchyme-free culture. *Dev Dyn* 222: 263–272

Qiao J, Bush KT, Steer DL, Stuart RO, Sakurai H, Wachsman W, Nigam SK (2001) Multiple fibroblast growth factors support growth of the ureteric bud but have different effects on branching morphogenesis. *Mech Dev* 109: 123–135

Qiao J, Sakurai H, Nigam SK (1999) Branching morphogenesis independent of mesenchymal-epithelial contact in the developing kidney. *Proc Natl Acad Sci USA* 96: 7330–7335

Ring DB, Johnson KW, Henriksen EJ, Nuss JM, Goff D, Kinnick TR, Ma ST, Reeder JW, Samuels I, Slabiak T, Wagman AS, Hammond ME, Harrison SD (2003) Selective glycogen synthase kinase 3 inhibitors potentiate insulin activation of glucose transport and utilization in vitro and in vivo. *Diabetes* 52: 588–595

Rosario M, Birchmeier W (2003) How to make tubes: signaling by the Met receptor tyrosine kinase. *Trends Cell Biol* 13: 328–335

Sakane H, Yamamoto H, Matsumoto S, Sato A, Kikuchi A (2012) Localization of glypican-4 in different membrane microdomains is involved in the regulation of Wnt signaling. *J Cell Sci* 125: 449–460

Sakaue-Sawano A, Kurokawa H, Morimura T, Hanyu A, Hama H, Osawa H, Kashiwagi S, Fukami K, Miyata T, Miyoshi H, Imamura T, Ogawa M, Masai H, Miyawaki A (2008) Visualizing spatiotemporal dynamics of multicellular cell-cycle progression. *Cell* 132: 487–498

Sakurai H, Barros EJ, Tsukamoto T, Barasch J, Nigam SK (1997) An in vitro tubulogenesis system using cell lines derived from the embryonic kidney shows dependence on multiple soluble growth factors. *Proc Natl Acad Sci USA* 94: 6279–6284

Santos OF, Nigam SK (1993) HGF-induced tubulogenesis and branching of epithelial cells is modulated by extracellular matrix and TGF-β. *Dev Biol* 160: 293–302

Santy LC, Ravichandran KS, Casanova JE (2005) The DOCK180/Elmo complex couples ARNO-mediated Arf6 activation to the downstream activation of Rac1. *Curr Biol* 15: 1749–1754

Sanz-Moreno V, Gadea G, Ahn J, Paterson H, Marra P, Pinner S, Sahai E, Marshall CJ (2008) Rac activation and inactivation control plasticity of tumor cell movement. *Cell* 135: 510–523

Saucedo LJ, Edgar BA (2007) Filling out the Hippo pathway. *Nat Rev Mol Cell Biol* 8: 613–621

Song R, Spera M, Garrett C, Yosypiv IV (2010) Angiotensin II-induced activation of c-Ret signaling is critical in ureteric bud branching morphogenesis. *Mech Dev* 127: 21–27

Steinberg Z, Myers C, Heim VM, Lathrop CA, Rebustini IT, Stewart JS, Larsen M, Hoffman MP (2005) FGFR2b signaling regulates ex vivo submandibular

gland epithelial cell proliferation and branching morphogenesis. *Development* 132: 1223 – 1234

Straight AF, Cheung A, Limouze J, Chen I, Westwood NJ, Sellers JR, Mitchison TJ (2003) Dissecting temporal and spatial control of cytokinesis with a myosin II Inhibitor. *Science* 299: 1743 – 1747

Tushir JS, D'Souza-Schorey C (2007) ARF6-dependent activation of ERK and Rac1 modulates epithelial tubule development. *EMBO J* 26: 1806 – 1819

Varelas X, Miller BW, Sopko R, Song S, Gregorieff A, Fellouse FA, Sakuma R, Pawson T, Hunziker W, McNeill H, Wrana JL, Attisano L (2010) The Hippo pathway regulates Wnt/β-catenin signaling. *Dev Cell* 18: 579 – 591

Wada K, Itoga K, Okano T, Yonemura S, Sasaki H (2011) Hippo pathway regulation by cell morphology and stress fibers. *Development* 138: 3907 – 3914

Watanabe T, Costantini F (2004) Real-time analysis of ureteric bud branching morphogenesis in vitro. *Dev Biol* 271: 98 – 108

Yamamoto H, Awada C, Hanaki H, Sakane H, Tsujimoto I, Takahashi Y, Takao T, Kikuchi A (2013) The apical and basolateral secretion of Wnt11 and Wnt3a in polarized epithelial cells is regulated by different mechanisms. *J Cell Sci* 126: 2931 – 2943

Yu W, O'Brien LE, Wang F, Bourne H, Mostov KE, Zegers MM (2003) Hepatocyte growth factor switches orientation of polarity and mode of movement during morphogenesis of multicellular epithelial structures. *Mol Biol Cell* 14: 748 – 763

Zeng Q, Hong W (2008) The emerging role of the hippo pathway in cell contact inhibition, organ size control, and cancer development in mammals. *Cancer Cell* 13: 188 – 192

Zhang X, Bush KT, Nigam SK (2012) In vitro culture of embryonic kidney rudiments and isolated ureteric buds. *Methods Mol Biol* 886: 13 – 21

